Hindawi
Advances in Materials Science and Engineering
Volume 2021, Article ID 5831721, 13 pages
https://doi.org/10.1155/2021/5831721

Research Article

The Normal Force Characteristic of a Novel Magnetorheological Elastomer Based on Butadiene Rubber Matrix Compounded with the Self-Fabricated Silly Putty

Fei Guo,[1] Chengbin Du ,[2] and Guojun Yu[3]

[1]*School of Civil Engineering and Architecture, Anhui Polytechnic University, Wuhu 241000, China*
[2]*Department of Engineering Mechanics, Hohai University, Nanjing 210098, China*
[3]*Faculty of Civil Engineering and Mechanics, Jiangsu University, Zhenjiang 212013, China*

Correspondence should be addressed to Chengbin Du; cbdu@hhu.edu.cn

Received 15 October 2021; Accepted 29 November 2021; Published 14 December 2021

Academic Editor: Rotana Hay

In this paper, a novel magnetorheological elastomer (MRE) was prepared by dispersing carbonyl iron particles (CIPs) into a composite matrix compounded by butadiene rubber (BR) and self-fabricated Silly Putty. The rate-sensitive and magneto-induced characteristics of normal force were experimental investigated to discuss the working mechanism. The results demonstrated that the normal force increased with the compression rate and the mass fraction of boron-silicon copolymer added to the composite matrix due to the formation of the more and more B-O cross bonds which could be blocked in the C-C cross-linked network of BR. Meanwhile, the magneto-induced normal force was positively correlated with the applied magnetic field strength and the compression strain due to the decreased gap between the centers of soft magnetic particles and the increased particle intensity of magnetization. Moreover, the magneto-induced normal force continued to enhance with the increase of compression strain because the CIP chains fixed in the C-C cross-linked network could bend to a radian and CIP chains in B-O cross-linked network could rupture to form more stable and intensive short-chain structures. Besides, a simplified model was deduced to characterize the mechanism of the generation of the magneto-induced normal force. Furthermore, the normal force varied stably with the oscillatory shear strain (less than 9%) at different magnetic induction intensities and suddenly reduced when the applied oscillatory shear strain was more than 9%.

1. Introduction

Magnetorheological elastomer (MRE) is an intelligent material by dispersing micron-sized carbonyl iron particles (CIPs) into traditional rubber or thermoplastic matrix uniformly [1–3]. Different applied magnetic field strengths can control the dynamic mechanical properties such as the obtained MRE's storage modulus and damping factor [4, 5]. Because of the exhibited magnetorheological effect, this intelligent and safe material can be widely used in dampers [6, 7], soft armors [8], impact absorbers [9–12], and other applications such as shielding [13, 14], force sensing [15, 16], and medical systems [17, 18]. However, due to the contradiction between the magnetorheological effect and mechanical properties induced by cross-linking degree of polymer rubber matrix [19], it is challenging to obtain MRE samples with excellent magnetorheological effect. Besides, MRE usually works in shear mode; the occurrence of shear behavior is perpendicular to the magnetic induction line direction, so the level of MRE shear modulus is far less than the vertical modulus. Furthermore, vertical extrusion deformation is limited; the tiny deformation can produce an excellent output strength. Therefore, it is essential to study the mechanical properties and magnetorheological effect of MRE in extrusion mode.

Silly Putty is a boron-silicon copolymer that can be stimulated to generate significant non-Newtonian behavior of shear stiffening performance. More nanocomposites based on Silly Putty have been intensively researched and discussed [20–22]. Xu et al. [23] fabricated a soft sandwich

structure consisting of two-layer Kevlar face sheets and a Silly Putty core. The results displayed that the storage modulus of Silly Putty, which was prepared by dispersing $CaCO_3$ particles into polyborodimethylsiloxane, increased by two to three orders of magnitude with the increasing shear frequency. The higher $CaCO_3$ content resulted in better shear-hardening behavior, which further enhanced the anti-impact performance of the sandwich structure. However, when micron-sized carbonyl iron particles (CIPs) are dispersed into Silly Putty, the properties of obtained magnetorheological Silly Putty (MRSP) can self-adapt to changes in the external stimuli environment and be controlled by different applied magnetic field strengths [24]. As a new kind of multifunctional material, it has aroused worldwide concern in recent years. Wang et al. [25] firstly prepared a novel multifunctional polymer composite (MPC) with different magnetic particles (CIP and Fe_3O_4), polydimethylsiloxane (PDMS), boric acid, and benzoyl peroxide (BPO). Besides, the mechanisms of "cross bonds" from the decomposition of cross-linking agent BPO and the magnetic particle chains induced by the magnetic field were introduced to describe the excellent multifunctional stimulus-response properties. Yao et al. [26] developed a novel magnet-induced aligning magnetorheological elastomer (MIMRE) based on ultrasoft polymeric matrix compounded of PDMS, boric acid, and chloroform to obtain the excellent magnetorheological effect and healing performance. Golinelli et al. [27] studied the behavior of magnetic Silly Putty first under a quasi-static compression and shear loading and second under dynamic shear loading; the results highlighted a strong dependence on the deformation rate the influence of the magnetic field was weak. However, in addition to applying single boron-silicon as the matrix, Wang [28] fabricated a novel magnetorheological shear-stiffening elastomer (MSTE) by dispersing CIPs into the shear-stiffening elastomer, which was synthesized by co-polymerization of shear-stiffening gel (STG) and methyl vinyl silicone rubber (VMQ). The results indicated that the content of STG could adjust the magnetic controllability and shear-stiffening performance of MSTE.

Besides, the influence factors and mechanisms of multifunctional properties for MRSP have also been extensively explored recently. Firstly, the rate-sensitive characteristic is mainly determined by the number of the B-O "cross bonds." Liu et al. [29] prepared multifunctional magnetorheological gel (MMRG) samples with the mass ratio of pyroboric acid to PDMS varying from 0 to 0.6. The results demonstrated that the shear stiffening performance was positively correlated with the number of "cross bonds," and when the numbers of molecular chains containing Si-O and Si-O-B were close (the mass ratio of pyroboric acid to PDMS reached 0.3), a substantial number of "cross bonds" were formed to result in excellent shear stiffening performance. Furthermore, the curing process, including temperature and time, were considered important factors influencing the shear stiffening performance [30]. In the study, curing temperature of 120°C and curing time of 30 min were selected to obtain the best shear stiffening performance. Moreover, additives such as $CaCo_3$ [31], graphene [32], and carbon nanotubes [33, 34] were invested in the promotion of rate-sensitive characteristics. Simultaneously, the magnetorheological effect of MRSP induced by the externally imposed magnetic field is generally influenced by magnetic saturation of particles, magnetic particle size and dispersion, matrix properties, and additives similar to other magnetorheological materials [35–39]. The mechanism of formed chain or column structures [40–43] for magnetic particles along magnetic induction lines was usually employed to describe the magnetorheological effect.

Therefore, in this work, a novel MRE was prepared by dispersing CIPs into the BR matrix with the addition of self-fabricated Silly Putty. The rheometer testing system studied the normal force characteristic of the synthetic novel composite MRE. The testing results revealed that the developed novel MRE exhibited excellent magnetorheological effect and rate-dependent performance in extrusion mode. Furthermore, the content of Silly Putty played a pivotal role in improving the axial deformation ability of the novel MRE.

2. Experimental Methods

2.1. Materials. PDMS, boric acid, and absolute ethyl alcohol, purchased from Sinopharm Chemical Reagent Co. Ltd., Shanghai, China, were applied to fabricate the Silly Putty as well as the silicon-boron copolymer. Butadiene rubber (BR), vulcanization system including cross-linking agent benzoyl peroxide (BPO), zinc oxide (ZnO), stearic acid (SA), and accelerant, purchased from Sinopharm Chemical Reagent Co. Ltd., Shanghai, China, were applied to synthesize the composite matrix of MRE with Silly Putty. CIPs with different average particle sizes of 3.15, 3.5, and 3.65 μm were purchased from Jiangsu Tianyi Ultra-fine Metal Powder Co. Ltd., Xuyi, China. Dioctyl phthalate (DOP), purchased from Sinopharm Chemical Reagent Co. Ltd., Shanghai, China, was used as the plasticizer. All the materials were analytically pure, and multifunctional properties were tested by MCR302 rheometer (Anton Paar Co., Austria).

MAT-3000S soft magnetic DC testing device was used to characterize the soft magnetic property of CIPs. The *B-H* magnetizing curves of different average particle sizes are displayed in Figure 1. It is shown that CIP with an average particle size of 3.5 μm exhibits the best soft magnetic performance, which presents lower coercivity H_c (only 93.61 A/m and testing magnetic field strength at 20,000 A/m) and the similar magnetization to CIP with an average size of 3.65 μm. Therefore, in this work, CIP with an average particle size of 3.5 μm was selected as the filling particles of the novel MRE samples to obtain the apparent magneto-induced property and reduce the effect of remanent magnetism. The performance indexes of the selected CIP are shown in Table 1.

2.2. Preparation and Properties of the Novel MRE Samples. The process of preparing the novel MRE sample is shown in Figure 2. The first heating process led to the formation of Silly Putty as well as the silicon-boron copolymer. The second step generates the composite matrix by mixing BR and Silly Putty. The last step formed the novel MRE sample

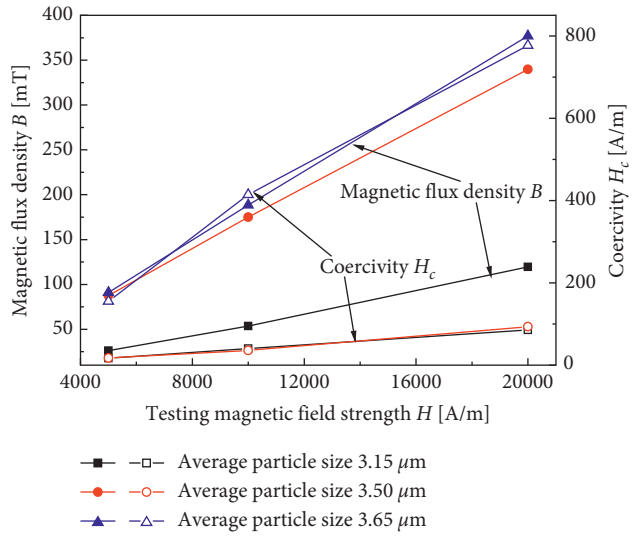

Figure 1: The testing *B-H* curve of CIPs with different average particle sizes.

Table 1: The major performance indexes of the CIP.

Fe content (%)	C content (%)	N content (%)	O content (%)	Average particle size (μm)	Apparent density	Tap density
98.10	0.74	0.90	0.26	3.5	2.8 g·cm^{-3}	4.25 g·cm^{-3}

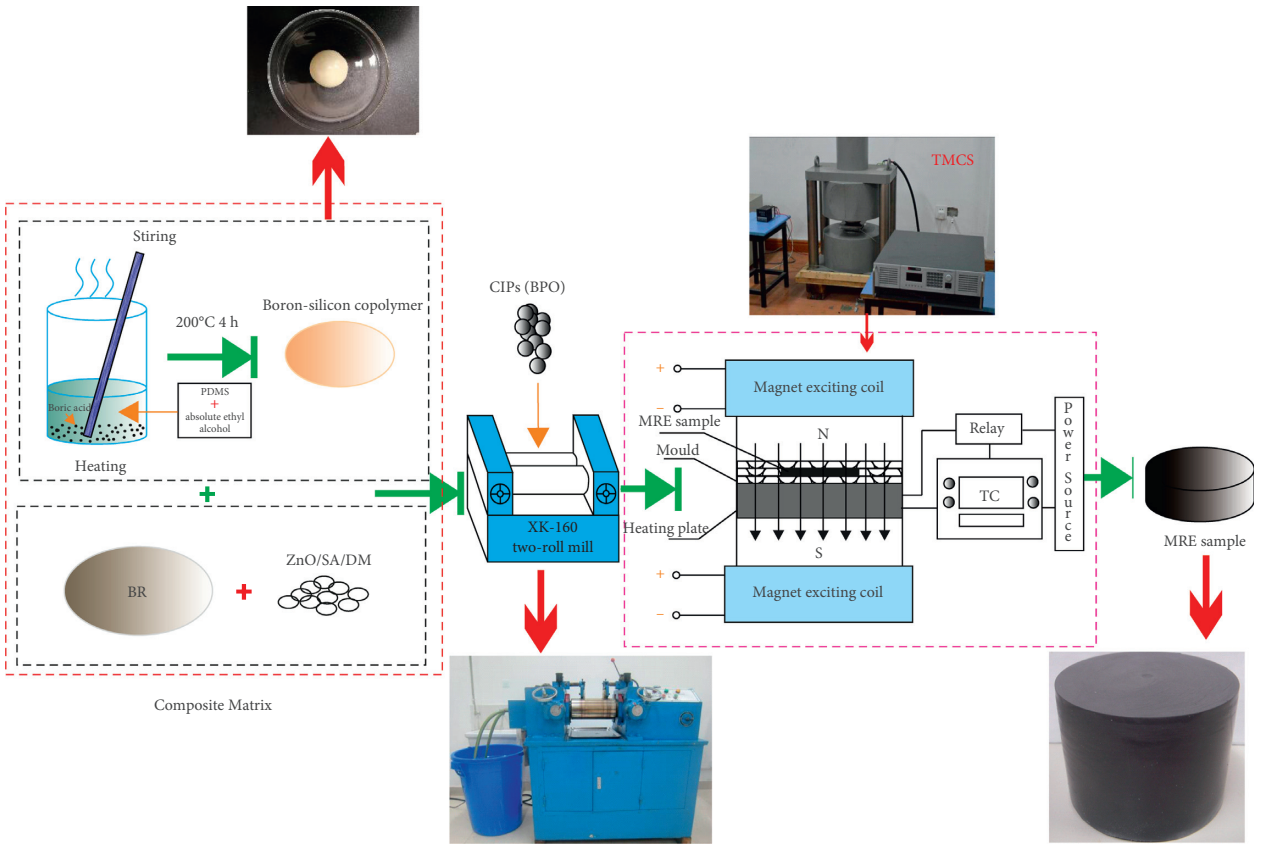

Figure 2: The preparation process of the novel MRE sample.

after the vulcanization process. The specific preparation steps were as follows:

(1) Firstly, the mixture of a certain amount of PDMS, boric acid, and absolute ethyl alcohol was stirred in a beaker at room temperature until homogeneously. Then, the mixture was heated at 200°C for 4 hours and stirred every 15 min to keep the reaction adequate. During the process, the Si-O bond was broken, and the Si-O-B bond was formed. The boron-silicon copolymer was obtained after the viscous mixture was cooled to room temperature.

(2) Next, the boron-silicon copolymer was mixed with BR in a two-roll mill (Nantong Hailite Rubber Machinery Inc., China; model XK-160) at room temperature. Additives such as ZnO, SA, accelerant, CIPs, and cross-linking agent BPO were added in sequence during the mechanical mixing method. Besides, plasticizer DOP was added in batches to improve the composite matrix plasticity.

(3) Finally, the compound was vulcanized at 120°C for 20 min in the thermal-magnetic coupling system (TMCS) to form the novel MRE sample. The TMCS consisted of magnet exciting coils, temperature controller (TC), external power source, heating plate, and a relay. The mixed unvulcanized MRE sample in the mold was placed on the heating plate to be cured to form the novel MRE between the magnetic induction lines generated by the two magnet exciting coils when the external current was input. The previous research demonstrated that prestructured MRE exhibited anisotropic characteristics and a more excellent magnetorheological effect [44] due to an increasing number of particle chains and columns formed in the matrix under the applied magnetic field. During the curing process, the magnetic induction intensity was constant at 1 T. The MRE sample was prepared when the product cooled down to room temperature.

In the preparation process, the amount of CIPs added to the novel MRE is stationary. Before the magnetic saturation, the higher the mass ratio of CIPs to the matrix, the more pronounced the magnetorheological effect is, and the more sensitive the material is to a magnetic field. However, excessive CIPs will increase the initial modulus of the MRE, thus reducing the relative magnetorheological effect and the regulation range induced by the magnetic field. Therefore, in this work, the mass fraction of CIPs remains at 75%. Four groups of MRE samples are fabricated, and the compositions of the four groups of MRE samples are listed in Table 2. According to the proportioning principle of the traditional rubber process, the composite matrix is set to 100 phr. The percent of Silly Putty to the composite matrix from MRE-1 to MRE-4 is 0%, 10%, 25%, and 40% in sequence, respectively. Hence, MRE-1 is based on the pure BR matrix. Besides, to the boron-silicon copolymer, the mass fraction of PDMS, boric acid, and the absolute ethyl alcohol is 80%, 15%, and 5%, respectively.

In this work, the Hitachi S4800 scanning electron microscope (SEM) was used to observe the internal microstructure of the MRE sample. The SEM images are displayed in Figures 3(a) and 3(b). It can be obtained from Figure 3(a) that CIPs are uniformly dispersed in composite matrix approximately, and the MRE sample presents isotropic feature when the prestructured magnetic field is in the close state. However, when the prestructured magnetic field is in the open state during the curing process, the CIPs are arranged in ordered chain structures along magnetic induction lines and MRE sample anisotropic feature from Figure 3(b).

The normal force characteristics of novel MRE samples were carried out by the MCR302 rheometer. During the testing procedure, a parallel plate PP20 with a diameter of 20 mm was used. The novel MRE sample was placed between the upper and lower plates. In this work, the normal force of each novel MRE sample was obtained by testing at quasi-static compression mode without magnetic field, quasi-static compression mode with the magnetic field, and dynamic oscillation shear mode. The rheological property of the fabricated boron-silicon copolymer is displayed in Figure 4. The fabricated Silly Putty exhibits apparent rate-sensitive performance. When the external rate-stimuli varies from 0 to 100 rad/s, the storage modulus of the boron-silicon copolymer generates the enhancement of three orders of magnitude.

3. Results and Discussion

3.1. The Normal Force at Quasi-Static Compression Mode without Magnetic Field. Under the condition of no external magnetic field and a constant compression rate, the normal force of the novel MRE samples on the rheometer plate can be detected. As for the fabricated four groups of the novel MRE samples from MRE-1 to MRE-4, Figure 5 shows the relationship between the normal force F_N and the gap h of parallel plates at the same compression rate of 100 μm/s. It is indicated that the normal force of all the MRE samples can reach the limit (50 N) of the rheometer when the samples are compressed to a specific state. Besides, as the mass fraction of the silicon-boron copolymer added in the matrix gradually increases, the compression deformation of the novel MRE samples gradually increases when it reaches the measurement limit of 50 N. For instance, the compression deformation of MRE-1 without the addition of silicon-boron copolymer is only 0.912 mm at the measured normal force limit of 50 N. However, the compression deformation of MRE-2 with the addition of 10% silicon-boron copolymer is 1.022 mm, while the compression of deformation of MRE-4 with the addition of silicon-boron copolymer exceeds 1.4 mm. It is because the modulus of the pure BR matrix is higher than the modulus of the silicon-boron copolymer. When the content of silicon-boron copolymer in the composite matrix is enhanced, the overall modulus of the novel MRE will reduce. Therefore, it depends on more significant compression deformation to achieve the same normal force. In addition, after each compression deformation, the novel MRE samples can generally recover to the initial deformation state. Hence, compared to the traditional MRE-1, it can improve the axial deformation capacity of the

Table 2: The composition of composite MRE samples (phr).

Samples	BR	Boron-silicon copolymer	CIPs	BPO	Vulcanization system, accelerant	ZnO	SA	DOP
MRE-1	100	0	645	5	5	3	2	100
MRE-2	90	10	645	5	5	3	2	100
MRE-3	75	25	645	5	5	3	2	100
MRE-4	60	40	645	5	5	3	2	100

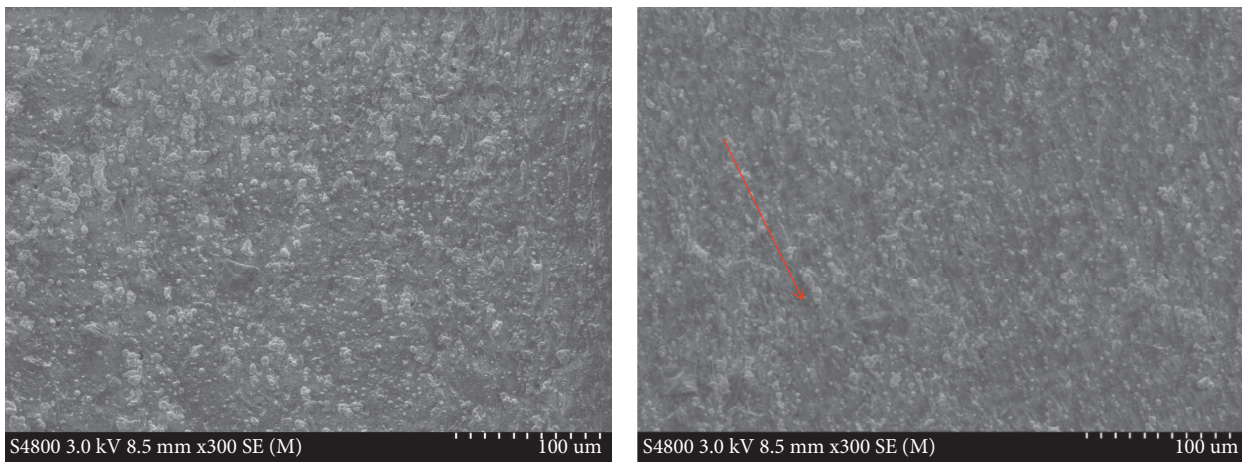

(a) (b)

Figure 3: Prepared MRE sample and SEM image of internal microstructure: (a) the prestructured magnetic field is in the close state and (b) the prestructured magnetic field is in the open state.

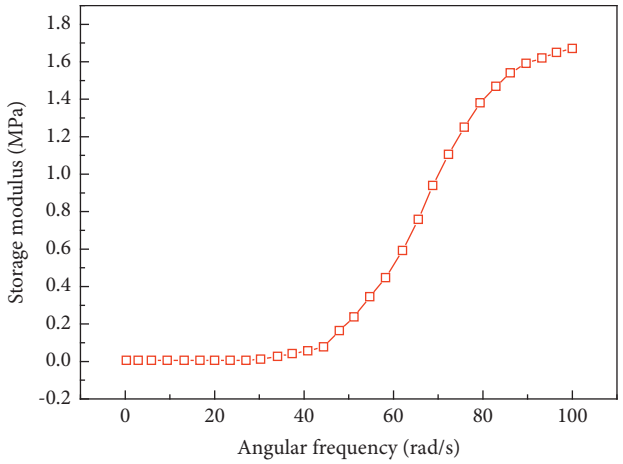

Figure 4: The rheological property of the fabricated boron-silicon copolymer.

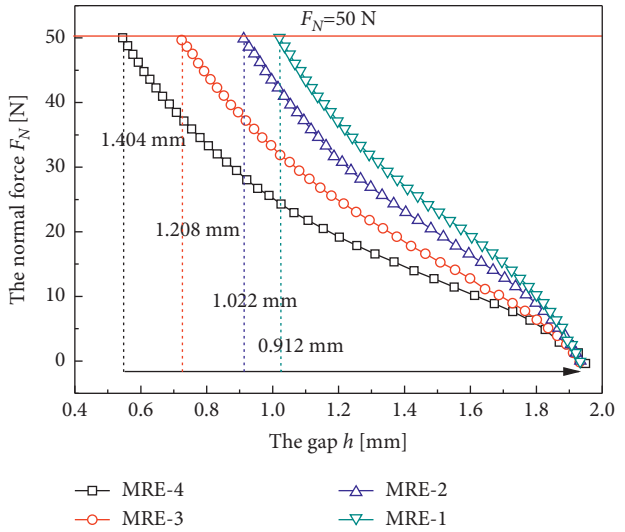

Figure 5: The normal force of the novel MRE samples as a function of the gap.

novel MRE samples by adjusting the content of the silicon-boron copolymer in the composite matrix.

Figures 6(a) and 6(b) show the relationship between the normal force and the gap of parallel plates at different compression rates of MRE-1 and MRE-4, respectively. The compression rate of 100, 200, 300, and 400 μm/s are applied separately in sequence, and the starting-ending positions of the compression range are the same. It can be observed from Figure 6(a) that the normal force curves of MRE-1 almost coincide under different compression rates. Furthermore, MRE-1 based on pure BR matrix exhibit no prominent rate-sensitive characteristic because the modulus of rubber only appears weak variation trend within an extensive exerted rate or frequency range. From Figure 6(b), MRE-4 exhibits prominent rate-sensitive property from the obtained normal force, increasing with the applied compression rate. When the compression deformation is 0.46 mm and the compression rate is 100 μm/s, the normal force of MRE-4 is only 12.7 N. However, when the compression rate reaches 400 μm/s, the normal force of MRE-4 can achieve 19.1 N,

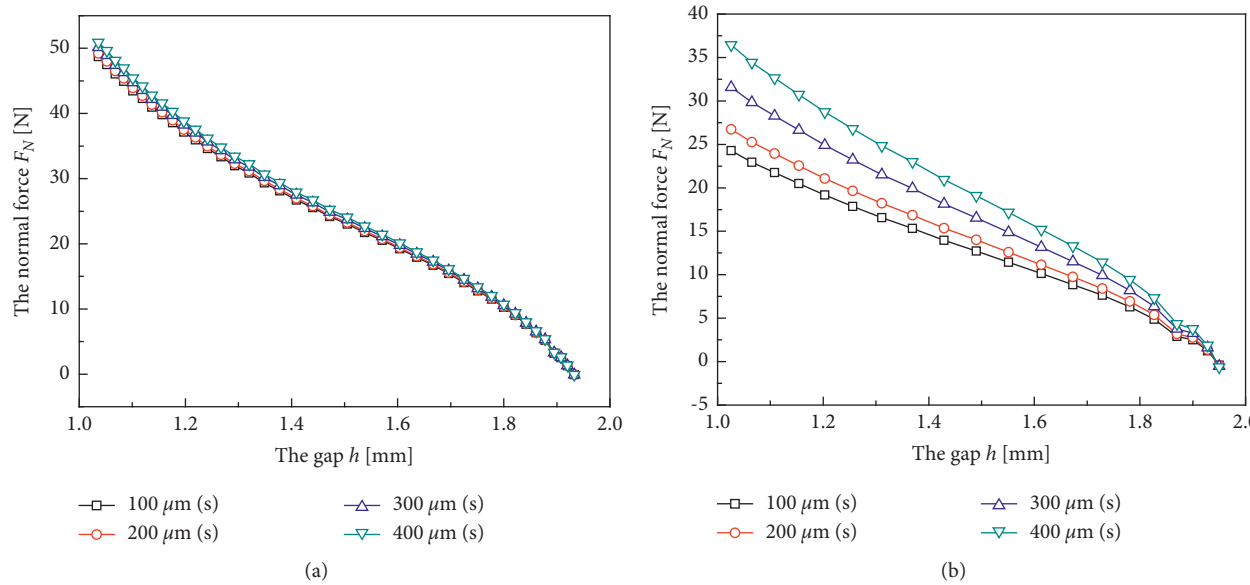

Figure 6: The normal force of the novel MRE samples as a function of the gap: (a) MRE-1 and (b) MRE-4.

which increases by 6.4 N dependently. While the compression deformation increases to 0.9 mm and the compression rate are 100 μm/s, the normal force of MRE-4 is just 24.3 N. As the compression rate increases to 400 μm/s, the normal force of MRE-4 can achieve 36.5 N, which increases 12.2 N dependently. Therefore, the novel MRE-4 sample with the addition of silicon-boron copolymer exhibits a more obvious rate-dependent performance of the normal force at more considerable compression deformation. Overall, the rate-sensitive property of the novel MRE can also reflect in the vertical normal force, not only in the horizontal shear performance based on the rheometer testing system.

From the working mechanism, the chain structure of PDMS has different polymerization degrees. When the PDMS reacts with boric acid, the Si-O bond breaks, and boron (atom B) is simultaneously introduced into the chains to form the silicon-boron copolymer with the Si-O-B bond. The molecular structure of the PDMS and the chains doped with atom B that can assume three forms [25, 45] are shown in Figure 7(a).

The electron-deficient p orbital of atom B obtains electrons from atom O in the Si-O bond [46] after forming the silicon-boron copolymer. Therefore, from Figure 7(b), the atom B from the Si-O-B bond in the chain structure of silicon-boron copolymer and the atom O from the Si-O bond in the chain structure of PDMS contribute to the formation of the B-O cross bond together that stimulate the rate-sensitive performance. In other words, the cross bond can be described as a slight damper, including a pair of piston and cylinder that can play an essential role in force output at different rate stimuli.

Furthermore, to the MRE sample based on pure BR matrix, the C-C cross bond can be formulated by adding cross-linking agent BPO, illustrated in Figure 8. The CIPs with chain structures are fixed in the cross-linked network formed by C-C cross bonds. However, when the silicon-boron copolymer is added to the BR matrix, the B-O cross bond will be blocked in the cross-linked network of BR [47] due to the tremendous C-C bond energy exhibited in the cube cell. As for the B-O cross bond, the B and O come from the silicon-boron copolymer; therefore, the percent of silicon-boron copolymer determines the number of B-O cross bonds. From Figure 8, when the percent of silicon-boron copolymer increases gradually, the number of B-O cross bonds will enhance dependently, exhibiting more obvious rate-sensitive characteristics macroscopically. Besides, when the lower compression rate is applied, more "pistons" from atom O and "cylinders" from atom B are active freely concerning a small amount of the B-O connected "damper." Therefore, the movement of chains is relatively free and flowing. When the compression rate increases, more and more "pistons" and "cylinders" are attracted to connect as "dampers," which generate more B-O cross bonds. Furthermore, the movement of chains with Si-O-Si bond and Si-O-B bond will be restricted due to gradually forming the B-O cross-linked network. Hence, the axial modulus and normal force will be improved with the applied compression rate.

3.2. The Normal Force at Quasi-Static Compression Mode with the Magnetic Field. When there is an external magnetic field and a constant compression rate applied, the normal force of the novel MRE samples on the rheometer plate can be detected by adjusting the magnetic field strength. The variation of normal force with the external magnetic field strength is an essential indicator of the magnetorheological effect of the novel MRE samples.

Figure 9 reveals the relationship between the normal force and the magnetic induction intensity of MRE-1 and MRE-4. The compression strain of 10%, 20%, 30%, 40%, and 50% is applied, and the magnetic induction intensity varies

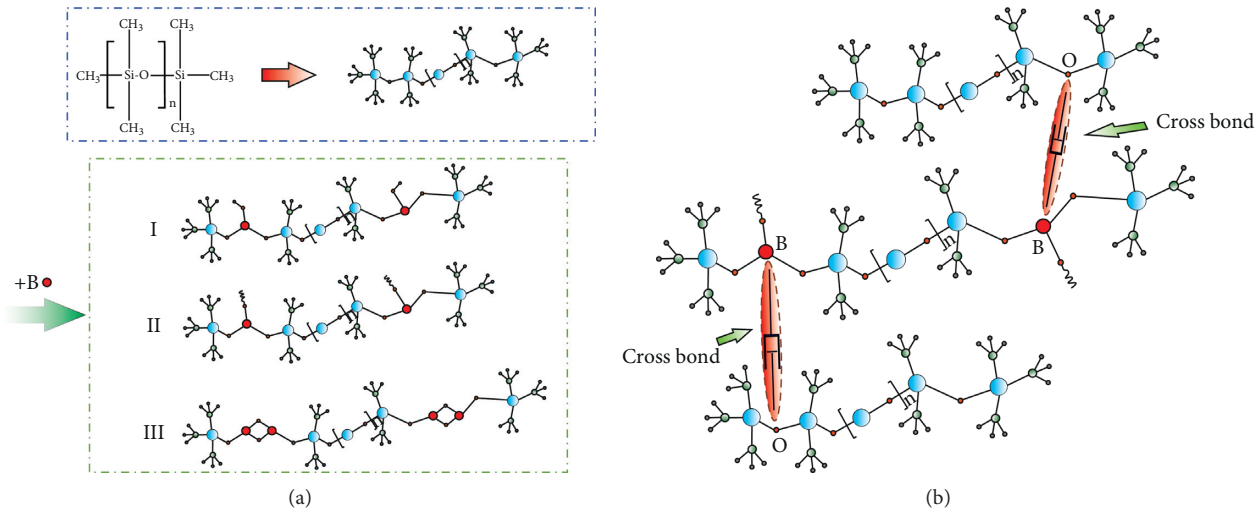

FIGURE 7: (a) Three possible structural forms of a molecular chain doped with atom B and (b) the mechanism to describe the formation of the cross bond.

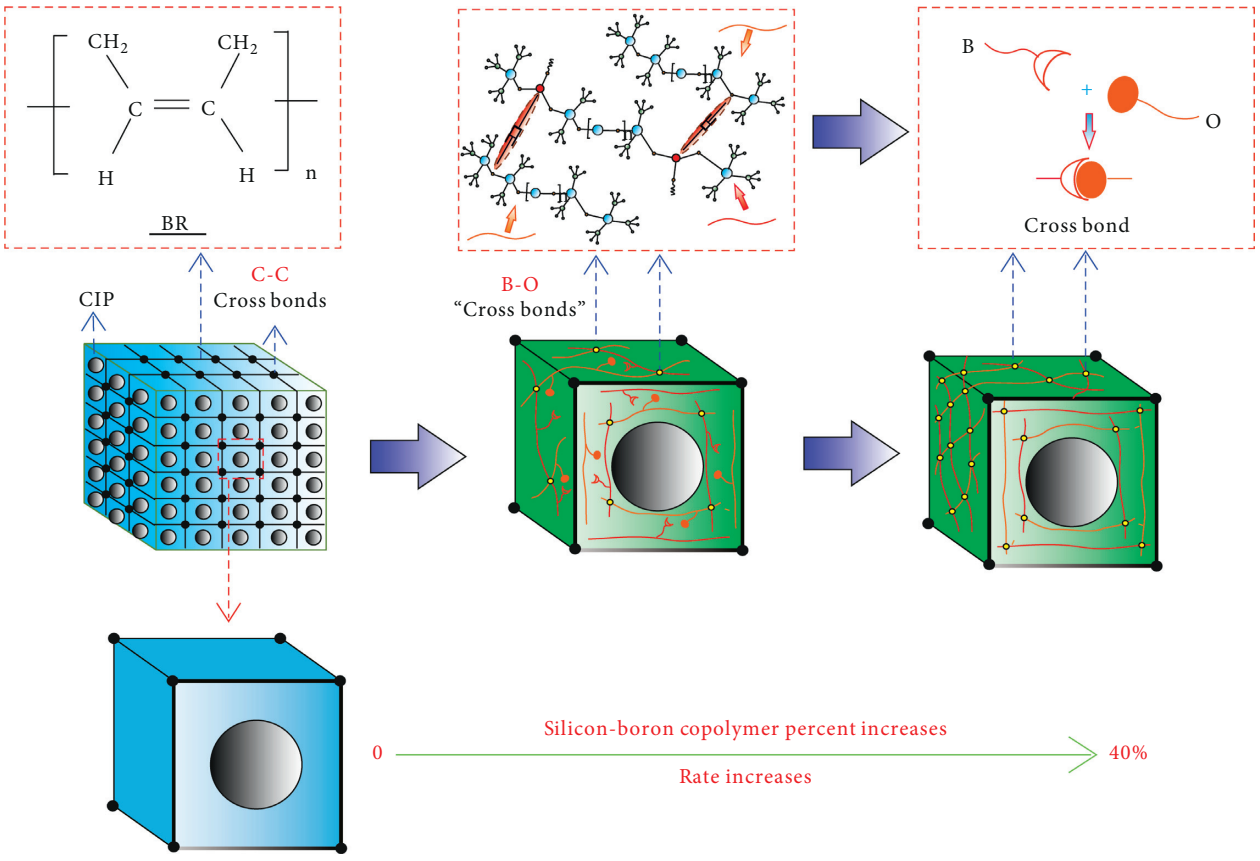

FIGURE 8: The mechanism of rate-sensitive characteristics and the molecular chain model when silicon-boron copolymer percent increases.

from 0 to 1.13 T continuously. It can be concluded that the normal force of each curve gradually increases with the enlargement of magnetic induction intensity, and when the magnetic induction intensity reaches 0.9 T, the normal force gradually tends to be stable due to magnetic saturation. Besides, compared with the traditional MRE-1 without the addition of Silly Putty, the overall normal force of MRE-4 at each compression strain is lower. However, the adjustable range of normal force for MRE-4 is more comprehensive than MRE-1 due to the greater initial normal force of MRE-1. For instance, when the compression strain is 30% and the magnetic induction intensity varies from 0 to 1.13 T, the normal force of MRE-4 can change from 14.2 to 18.9 N, and the relative rate is 33%, which is greater than 21% of MRE-1.

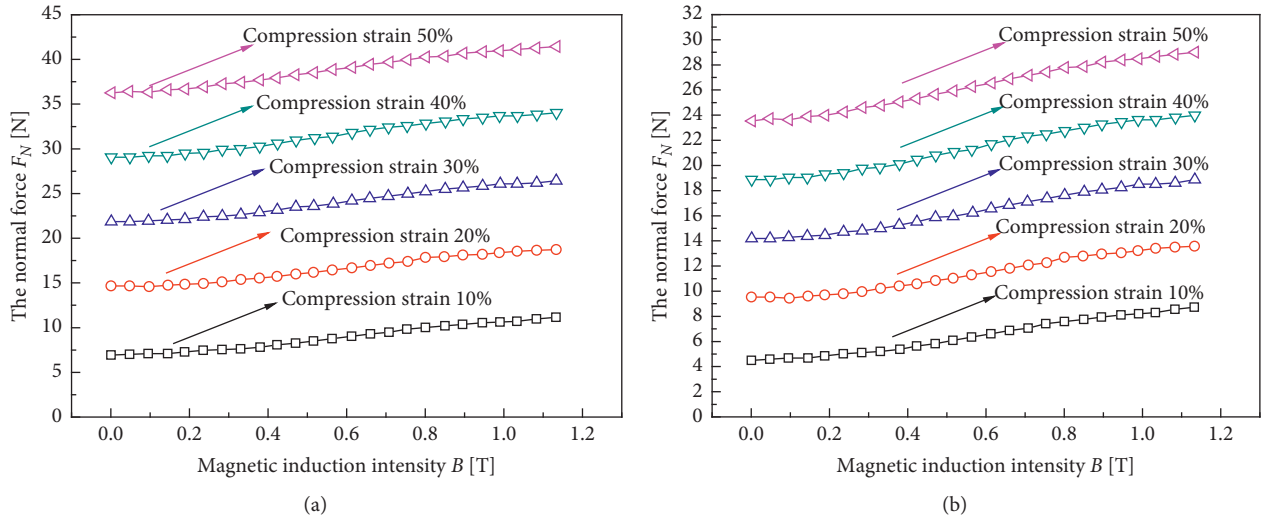

Figure 9: The normal force as a function of magnetic induction intensity at different compression strains: (a) MRE-1 and (b) MRE-4.

Therefore, it is explicit that the addition of Silly Putty can improve the adjustable range of normal force with magnetic field for MRE samples.

Figure 10 shows the relationship between the magneto-induced normal force ΔF_N and compression strain of MRE-4 at different magnetic induction intensities. Obviously, on the same compressive strain condition, the magneto-induced normal force increases with the magnetic induction intensity and tends to magnetic saturation when the magnetic induction intensity attains 0.997 T. Meanwhile, the variation trend between magneto-induced normal force and compression strain at different magnetic induction intensities is the same. When the compression strain is less than 20%, the magneto-induced normal force at different magnetic induction intensities is almost constant. Besides, when the compression strain is more than 20%, the magneto-induced normal force at different magnetic induction intensities increases with the increase of the compression strain. Furthermore, when the magnetic induction intensity attains to 1.03 T and the compression strain is 10%, the maximum magneto-induced normal force to magnetic saturation is 3.8 N. By comparison, the maximum magneto-induced normal force at the compression strain of 50% is more remarkable than 5 N.

Similar to the shear stress of MRE, the normal force is derived from the composite matrix and the interaction between the soft magnetic particles, which can be expressed as ΔF_N. The saturation magnetization intensity is the apparent property of soft magnetic particles. Therefore, when the magnetic induction intensity increases gradually, the soft magnetic particles are magnetized until they reach saturation. Due to the apparent nonlinear property of the magnetized process, the magneto-induced normal force of novel MRE samples exhibits evident nonlinear characteristics.

The magneto-induced mechanism can be described in Figure 11. To the prestructured MRE sample, the CIPs are arranged in chain structures along the magnetic induction line fixed in the composite matrix compounded by BR and Silly Putty. When the external compression force F is applied, the composite matrix can be compressed to deformation. Meanwhile, the gap d between the centers of particles will reduce until the adjacent particles contact. However, when the compression deformation continues to increase to the particles fixed in the BR cross-linked network, the particle chains will bend to a possible radian due to compression force f. Still, to the particles in the Silly Putty, the long particle chains probably tend to rupture to form more intensive and stable short particle chains, which can generate more obvious magneto-induced normal force.

During the process of particle gap reduction, a simplified model based on the magnetic dipole and coupling field theory can be concluded to describe the magneto-induced normal force ΔF_N. In this model, CIPs are simplified to spheres with the same radius r. For a dipole i in a chain, its magnetic dipole moment can be expressed as follows [48]:

$$\vec{m}_i = \frac{4}{3}\pi r^3 \mu_0 \mu_1 M = \frac{4}{3}\pi r^3 \mu_0 \mu_1 \chi H_i, \tag{1}$$

where permeability of vacuum $\mu_0 = 4\pi * 10^{-7}$, μ_1 is the relative permeability of composite matrix, χ is the magnetic susceptibility, and M is the magnetization of a soft magnetic particle that can achieve magnetic saturation M_s during nonlinear magnetization.

The magnetic field strength at particle i can be expressed as follows [49]:

$$H_i = \vec{H}_0 + \sum_{j \neq i} H_j = \vec{H}_0 + 2\sum_{j=1}^{n} \frac{3\hat{d}\left(\hat{d} \cdot \vec{m}_j\right) - \vec{m}_j}{4\pi\mu_0\mu_1\left(d_j\right)^3}, \tag{2}$$

where $\vec{H}_0$ is the external magnetic field strength, $\hat{d}_j$ is the unit vector of $\vec{d}_j$, and $d_j = jd$. Substitute equation (1) into (2) to get

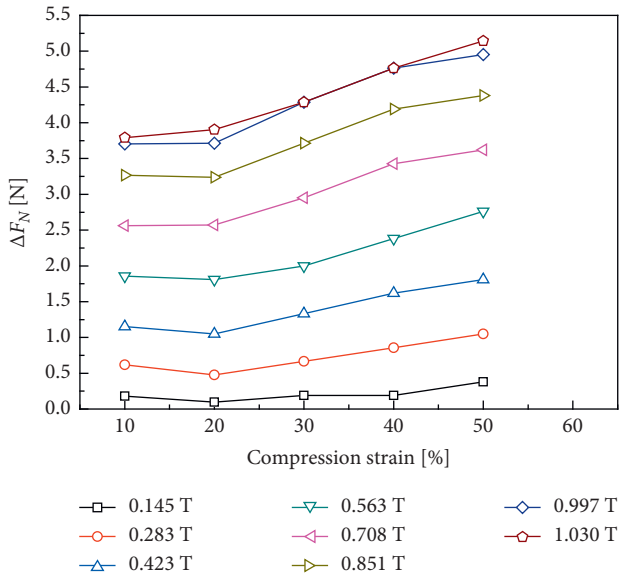

Figure 10: The magneto-induced normal force as a function of compression strain for MRE-4.

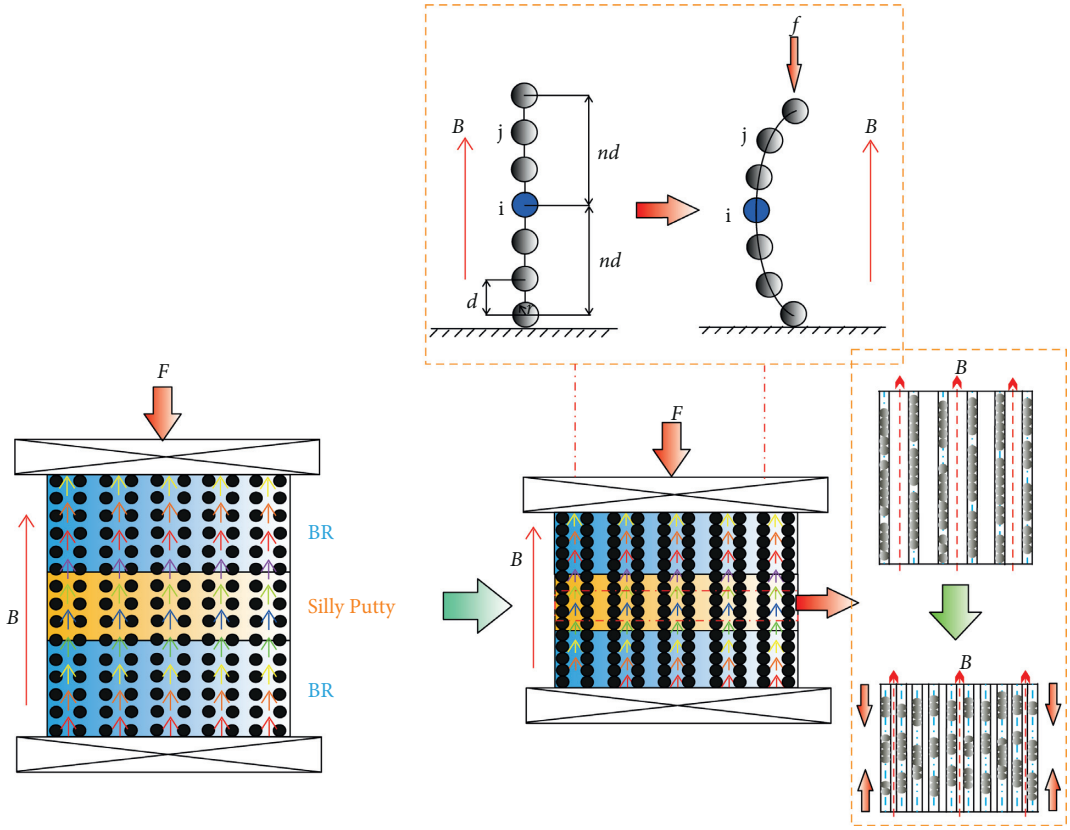

Figure 11: The magneto-induced mechanism of the novel MRE when compression is applied.

$$\vec{m}_i = \frac{4}{3}\pi r^3 \mu_0 \mu_1 \chi \left[H_0 + 2 \sum_{j=1}^{n} \frac{3\hat{d}\left(\hat{d} \cdot \vec{m}_j\right) - \vec{m}_j}{4\pi\mu_0\mu_1 (j\ d)^3} \right], \tag{3}$$

where assume $A = \sum_{j=1}^{n} 1/j^3$; when n is large enough, $A \approx 1.202$.

Moreover, the compression strain can be expressed as follows:

$$\varepsilon = \frac{d - d_0}{d}, \tag{4}$$

where d_0 is the initial distance between adjacent particles. Because the stiffness of the soft magnetic particles is much larger than that of the composite matrix, the deformation of the particles can be ignored. Assume $m_i = m_j = m$, according to equation (3),

$$m = \frac{4}{3}\pi r^3 \mu_0 \mu_1 \chi H_0 \left[\frac{1}{1 - (4/3)\chi A (r/d)^3} \right]. \tag{5}$$

The magnetic interaction energy between the soft magnetic particle i and other soft magnetic particles in the same chain is

$$E = \frac{-1}{4\pi\mu_0\mu_1} \cdot \frac{4Am^2}{d^3}. \tag{6}$$

Therefore, the magnetic interaction energy per unit volume of the novel MRE can be expressed as follows:

$$E_d = \frac{3\phi}{8\pi r^3} E, \tag{7}$$

where ϕ is the volume fraction of the CIPs.

Hence, the magneto-induced normal stress can be expressed as follows:

$$\sigma = \frac{\partial E_d}{\partial \varepsilon} = \frac{\partial E_d}{\partial \mathrm{d}} \frac{\partial \mathrm{d}}{\partial \varepsilon} = d_0 \frac{\partial E_d}{\partial \mathrm{d}}. \tag{8}$$

The magneto-induced normal force can be expressed as the product of the normal stress and the cross-sectional area S as follows:

$$\Delta F_N = \sigma S. \tag{9}$$

When the soft magnetic particles reach the magnetic saturation M_s, according to equations (6)–(9), the maximum magneto-induced normal force of the novel MRE based on the composite matrix can be obtained as follows:

$$\Delta F_N = \frac{2Sd_0\phi A r^3 \mu_0 M_s^2}{\mu_1 d^4}. \tag{10}$$

From equation (10), the magneto-induced mechanism can be concluded that the magneto-induced normal force will enhance when the distance d between the centers of soft magnetic particles reduces with the increasing compression strain. Furthermore, the magneto-induced normal force will also enhance with the applied external magnetic field strength until the magnetic saturation of particles.

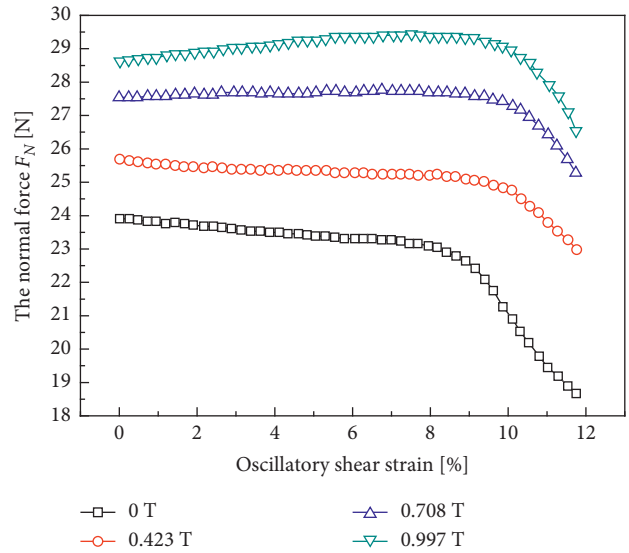

Figure 12: The normal force of MRE-4 at oscillatory shear mode.

3.3. The Normal Force at Dynamic Oscillation Shear Mode. The magnetic interaction between CIPs fixed in the matrix is the source of generation for magneto-induced shear stress and magneto-induced normal force. The previous research results reveal that in the process of shear deformation, the elastic modulus in the direction of compression and the torque applied to particle chains are two important influence factors to the normal force of MRE [50, 51]. Besides, the variation trends of the normal force caused by the two influence factors are the opposite [52, 53]. On the low magnetic field condition, the influence of elastic modulus in compressive direction is more evident than the torque applied to particle chains, so the normal force decreases with the increase of shear strain. However, the torque applied to particle chains gradually increases with the enhancement of the external magnetic field. Meanwhile, the enhancement of normal force caused by the increase of the torque is higher than the decrease of the normal force caused by the decrease of the elastic modulus in the compressive direction. So the normal force gradually increases with the enhancement of the shear strain on the condition of a high magnetic field.

Figure 12 presents the relationship between the normal force and oscillatory shear strain of MRE-4 at different magnetic induction intensities when the angular frequency of 10 rad/s is applied. The normal force is stable at different magnetic induction intensities when the oscillatory shear strain is less than 9%. However, when the oscillatory shear strain is more than 9%, the normal force sharply reduces regardless of the magnetic induction intensity. Most particle chains in MRE rupture suddenly, which can be replaced by the failure of particle chains that is more likely to occur in the oscillatory shear mode. Furthermore, the normal force further decreases with the enhancement of oscillatory shear strain due to the continuous fracture of particle chain structures.

4. Conclusions

A novel MRE based on composite matrix compounded by BR and self-fabricated Silly Putty was prepared. The normal force of MRE samples at quasi-static compression mode without magnetic field, quasi-static compression mode with the magnetic field, and dynamic oscillation shear mode were tested.

(1) The novel MRE samples with the addition of Silly Putty exhibited greater axial deformation capacity than traditional MRE-1. It could improve the novel MRE samples' axial deformation capacity by adjusting the silicon-boron copolymer's content in the composite matrix. Moreover, the normal force varied stably with the oscillatory shear strain (less than 9%) at different magnetic induction intensities and suddenly reduced when the applied oscillatory shear strain was more than 9%.

(2) The fabricated novel MRE-4 exhibited prominent rate-sensitive characteristics, indicating that normal force F_N enhanced with the increased compression rate than traditional MRE-1. The B-O cross bonds were formulated and blocked in the C-C cross-linked network of BR with the addition of silicon-boron copolymer. The more and more B-O cross bonds allowed the linear molecular chains to form a B-O cross-linked network structure that restricted the movement of molecular chains, including Si-O and Si-O-B bonds, resulting in an increase in the normal force the compression rate and the mass fraction of silicon-boron copolymer addition increased.

(3) Furthermore, compared to the traditional MRE-1, the addition of Silly Putty to the novel MRE samples could improve the adjustable range of normal force with the applied magnetic field. The magneto-induced normal force ΔF_N was obtained and increased with the magnetic induction intensity until magnetic saturation. Due to the prestructured CIP chains fixed in the composite matrix, the magneto-induced normal force was obtained under the applied external magnetic field. The gap d between the centers of soft magnetic particles reduced with the compression deformation, resulting in a slight increase of magneto-induced normal force. Moreover, when the compression deformation continued to increase, the CIP chains fixed in the C-C cross-linked network possibly bent to a radian, and the CIP chains in the B-O cross-linked network tended to rupture to form more intensive and stable short particle chains; therefore, the magneto-induced normal force increased. Besides, a simplified model was deduced to characterize the magneto-induced mechanism during the process of particles gap reduction. Furthermore, external magnetic field strength, gap d between the centers of soft magnetic particles, and magnetic saturation M_s were the key factors influencing the magneto-induced normal force ΔF_N.

Data Availability

The experimental data used to support the findings of this study are included within the article.

Conflicts of Interest

The authors declare that there are no conflicts of interest regarding the publication of this paper.

Acknowledgments

This work was supported by the Ph.D. Research Startup Foundation of Anhui Polytechnic University (Grant no. S022020069), the Key Research Foundation of Anhui Polytechnic University (Grant no. KZ42020240), and the Jiangsu Province Key R&D Project (Grant no. BE2017167).

References

[1] X. L. Gong, X. Z. Zhang, and P. Q. Zhang, "Fabrication and characterization of isotropic magnetorheological elastomers," *Polymer Testing*, vol. 24, no. 5, pp. 669–676, 2005.

[2] M. Cvek, M. Kracalik, M. Sedlacik, M. Mrlik, and V. Sedlarik, "Reprocessing of injection-molded magnetorheological elastomers based on TPE matrix," *Composites Part B: Engineering*, vol. 172, pp. 253–261, 2019.

[3] X. Qiao, X. Lu, X. Gong, T. Yang, K. Sun, and X. Chen, "Effect of carbonyl iron concentration and processing conditions on the structure and properties of the thermoplastic magnetorheological elastomer composites based on poly (styrene-b-ethylene-co-butylene-b-styrene) (SEBS)," *Polymer Testing*, vol. 47, pp. 51–58, 2015.

[4] Q. Shu, L. Ding, and T. Hu, "High performance magnetorheological elastomers strengthened by perpendicularly interacted flax fiber and carbonyl iron chains," *Smart Materials and Structures*, vol. 29, no. 2, pp. 25010–25013, 2020.

[5] F. Guo, C. B. Du, and R. P. Li, "Viscoelastic parameter model of magnetorheological elastomers based on abel dashpot," *Advances in Mechanical Engineering*, vol. 6, Article ID 629386, 2014.

[6] S. Sun, J. Yang, T. Yildirim et al., "A magnetorheological elastomer rail damper for wideband attenuation of rail noise and vibration," *Journal of Intelligent Material Systems and Structures*, vol. 31, no. 2, pp. 220–228, 2019.

[7] Q. Wang, X. F. Dong, L. Y. Li, and Q. Yang, "Wind-induced vibration control of a constructing bridge tower with MRE variable stiffness tuned mass damper," *Smart Materials and Structures*, vol. 29, no. 4, Article ID 045043, 2020.

[8] T. J. Kang, K. H. Hong, and H. Jeong, "Preparation and properties of a p -aramid fabric composite impregnated with a magnetorheological fluid for body armor applications," *Polymer Engineering & Science*, vol. 55, no. 4, pp. 729–734, 2015.

[9] Y. Wen, Q. Sun, Y. Zou, and H. You, "Study on the vibration suppression of a flexible carbody for urban railway vehicles with a magnetorheological elastomer-based dynamic vibration absorber," *Proceedings of the Institution of Mechanical Engineers, Part F: Journal of Rail and Rapid Transit*, vol. 234, no. 7, pp. 749–764, 2019.

[10] S. Sun, J. Yang, T. Yildirim et al., "Development of a nonlinear adaptive absorber based on magnetorheological elastomer," *Journal of Intelligent Material Systems and Structures*, vol. 29, no. 2, pp. 194–204, 2018.

[11] D. I. Jang, J. E. Park, and Y. K. Kim, "Designing a compact module of vibration absorber based on magnetorheological elastomer with a novel magnetic field generator," *Transactions of the Korean Society of Mechanical Engineers - A*, vol. 43, no. 3, pp. 177–183, 2019.

[12] A. Rasooli, R. Sedaghati, and M. Hemmatian, "A novel magnetorheological elastomer-based adaptive tuned vibration absorber: design, analysis and experimental characterization," *Smart Materials and Structures*, vol. 29, no. 11, Article ID 115042, 2020.

[13] M. Sedlacik, M. Mrlik, V. Babayan, and V. Pavlinek, "Magnetorheological elastomers with efficient electromagnetic shielding," *Composite Structures*, vol. 135, pp. 199–204, 2016.

[14] I. E. Kuznetsova, V. V. Kolesov, A. S. Fionov, and E. Y. Kramarenko, "Magnetoactive elastomers with controllable radio-absorbing properties," *Materials Today Communications*, vol. 21, Article ID 100610, 2019.

[15] M. Cvek, M. Mrlík, M. Ilčíková, J. Mosnáček, L. Münster, and V. Pavlínek, "Synthesis of silicone elastomers containing silyl-based polymer-grafted carbonyl iron particles: an efficient way to improve magnetorheological, damping, and sensing performances," *Macromolecules*, vol. 50, no. 5, pp. 2189–2200, 2017.

[16] B. Sapiński and P. Orkisz, "Real-time sensing action of the electromagnetic vibration-based energy harvester for a magnetorheological damper control," *Energies*, vol. 14, no. 10, Article ID 2845, 2021.

[17] M. Cvek, A. Zahoranova, M. Mrlik, P. Sramkova, A. Minarik, and M. Sedlacik, "Poly (2-oxazoline)-based magnetic hydrogels: synthesis, performance and cytotoxicity," *Colloids and Surfaces B: Biointerfaces*, vol. 190, Article ID 110912, 2020.

[18] N. M. Hapipi, S. A. Mazlan, U. Ubaidillah et al., "Solvent dependence of the rheological properties in hydrogel magnetorheological plastomer," *International Journal of Molecular Sciences*, vol. 21, no. 5, Article ID 1793, 2020.

[19] L. Chen, X. L. Gong, W. Q. Jiang, J. J. Yao, H. X. Deng, and W.H Li, "Investigation on magnetorheological elastomers based on natural rubber," *Journal of Materials Science*, vol. 42, no. 14, pp. 5483–5489, 2007.

[20] Z. Chang, Y. He, H. Deng et al., "A multifunctional silly-putty nanocomposite spontaneously repairs cathode composite for advanced Li–S batteries," *Advanced Functional Materials*, vol. 28, no. 50, Article ID 1804777, 2018.

[21] M. Hébert, J. P. Huissoon, and C. L. Ren, "A silicone-based soft matrix nanocomposite strain-like sensor fabricated using graphene and silly putty," *Sensors and Actuators A Physical*, vol. 305, no. 11, Article ID 111917, 2020.

[22] Y. Chen, X. Pu, M. Liu et al., "Shape-Adaptive, self-healable triboelectric nanogenerator with enhanced performances by soft solid-solid contact electrification," *ACS Nano*, vol. 13, no. 8, pp. 8936–8945, 2019.

[23] C. Xu, Y. Wang, J. Wu et al., "Anti-impact response of Kevlar sandwich structure with silly putty core," *Composites Science and Technology*, vol. 153, pp. 168–177, 2017.

[24] F. Guo, C. B. Du, G. J. Yu, and L. P. Run, "The static and dynamic mechanical properties of magnetorheological silly putty," *Advances in Materials Science and Engineering*, vol. 2016, Article ID 7079698, 11 pages, 2016.

[25] S. Wang, W. Jiang, W. Jiang et al., "Multifunctional polymer composite with excellent shear stiffening performance and magnetorheological effect," *Journal of Materials Chemistry C*, vol. 2, no. 34, pp. 7133–7140, 2014.

[26] J. Yao, Y. Sun, Y. Wang, Q. Fu, Z. Xiong, and Y. Liu, "Magnet-induced aligning magnetorheological elastomer based on ultra-soft matrix," *Composites Science and Technology*, vol. 162, no. 7, pp. 170–179, 2018.

[27] N. Golinelli, A. Spaggiari, and E. Dragoni, "Mechanical behaviour of magnetic Silly Putty: viscoelastic and magnetorheological properties," *Journal of Intelligent Material Systems and Structures*, vol. 28, no. 8, pp. 953–960, 2017.

[28] Y. Wang, L. Ding, C. Zhao et al., "A novel magnetorheological shear-stiffening elastomer with self-healing ability," *Composites Science and Technology*, vol. 168, no. 10, pp. 303–311, 2018.

[29] B. Liu, C. Du, G. Yu, and Y. Fu, "Shear thickening effect of a multifunctional magnetorheological gel: the influence of cross-linked bonds and solid particles," *Smart Materials and Structures*, vol. 29, no. 1, Article ID 015004, 2020.

[30] B. Liu, C. Du, S. Jiang, G. Zhou, and J. Sun, "The influence of the curing process on the shear thickening performance of RMG and property optimization," *RSC Advances*, vol. 10, no. 21, Article ID 12197, 2020.

[31] W. Jiang, X. Gong, S. Wang et al., "Strain rate-induced phase transitions in an impact-hardening polymer composite," *Applied Physics Letters*, vol. 104, no. 12, Article ID 121915, 2014.

[32] C. S. Boland, U. Khan, G. Ryan et al., "Sensitive electromechanical sensors using viscoelastic graphene-polymer nanocomposites," *Science*, vol. 354, no. 6317, pp. 1257–1260, 2016.

[33] X. Fan, S. Wang, S. Zhang, Y. Wang, and X. Gong, "Magnetically sensitive nanocomposites based on the conductive shear-stiffening gel," *Journal of Materials Science*, vol. 54, no. 9, pp. 6971–6981, 2019.

[34] M. Liu, S. Zhang, S. Liu et al., "CNT/STF/Kevlar-based wearable electronic textile with excellent anti-impact and sensing performance," *Composites Part A: Applied Science and Manufacturing*, vol. 126, no. 11, Article ID 105612, 2019.

[35] X. L. Gong, X. Z. Zhang, and P. Q. Zhang, "Study of mechanical behavior and microstructure of magnetorheological elastomers," *International Journal of Modern Physics B*, vol. 19, no. 7–9, pp. 1304–1310, 2005.

[36] Y. Wang, Y. Hu, L. Chen et al., "Effects of rubber/magnetic particle interactions on the performance of magnetorheological elastomers," *Polymer Testing*, vol. 25, no. 2, pp. 262–267, 2006.

[37] L. Pei, H. Pang, X. Ruan, X. Gong, and S. Xuan, "Magnetorheology of a magnetic fluid based on Fe_3O_4 immobilized SiO_2 core-shell nanospheres: experiments and molecular dynamics simulations," *RSC Advances*, vol. 7, no. 14, pp. 8142–8150, 2017.

[38] Q. Wen, Y. Wang, and X. Gong, "The magnetic field dependent dynamic properties of magnetorheological elastomers based on hard magnetic particles," *Smart Materials and Structures*, vol. 26, no. 7, Article ID 075012, 2017.

[39] W. Zhao, H. Pang, and X. Gong, "Novel magnetorheological plastomer filled with NdFeB particles: preparation, characterization, and magnetic-mechanic coupling properties," *Industrial & Engineering Chemistry Research*, vol. 56, no. 31, pp. 8857–8863, 2017.

[40] F. H. Xu, Z. D. Xu, X. C. Zhang, G. Q. Ying, and Y. Lu, "A compact experimentally validated model of magnetorheological fluids," *Journal of Vibration and Acoustics-Transactions of the ASME.*vol. 138, no. 1, Article ID 011017, 2016.

[41] W. H. Li, X. Z. Zhang, and T. F. Tian, "Fabrication and characterisation of patterned magnetorheological elastomers," *AIP Conference Proceedings*, vol. 1542, no. 1, pp. 129–132, 2013.

[42] W. Zhang, X. L. Gong, and L. Chen, "A Gaussian distribution model of anisotropic magnetorheological elastomers," *Journal of Magnetism and Magnetic Materials*, vol. 322, no. 23, pp. 3797–3801, 2010.

[43] Y. S. Zhu, X. L. Gong, H. Dang, X. Z. Zhang, and P. Q. Zhang, "Numerical analysis on magnetic-induced shear modulus of magnetorheological elastomers based on multi-chain model," *Chinese Journal of Chemical Physics*, vol. 19, no. 2, pp. 126–130, 2006.

[44] L. Chen, X. L. Gong, and W. H. Li, "Microstructures and viscoelastic properties of anisotropic magnetorheological elastomers," *Smart Materials and Structures*, vol. 16, no. 6, pp. 2645–2650, 2007.

[45] T. I. Zatsepina, M. L. Brodskii, Y. A. Frolova, A. A. Trapeznikov, V. N. Gruber, and G. A. Kruglova, "Rheological behaviour of polyheterosiloxanes," *Polymer Science U.S.S.R.*vol. 12, no. 11, pp. 2899–2905, 1970.

[46] M. P. Goertz, X.-Y. Zhu, and J. E. Houston, "Temperature dependent relaxation of a "solid-liquid"," *Journal of Polymer Science Part B: Polymer Physics*, vol. 47, no. 13, pp. 1285–1290, 2009.

[47] W. L. Wu and G. Cheng, "Study on silicone rubber/BR/EPDM blend," *China Elastomerics*, vol. 16, no. 1, pp. 43–46, 2006.

[48] M. R. Jolly, J. D. Carlson, and B. C. Muñoz, "A model of the behaviour of magnetorheological materials," *Smart Materials and Structures*, vol. 5, no. 5, pp. 607–614, 1996.

[49] Y. Shen, M. F. Golnaraghi, and G. R. Heppler, "Experimental research and modeling of magnetorheological elastomers," *Journal of Intelligent Material Systems and Structures*, vol. 15, no. 1, pp. 27–35, 2004.

[50] E. M. James and A. A. Robert, "Chain model of electrorheology," *The Journal of Chemical Physics*, vol. 104, no. 12, p. 4814, 1996.

[51] J. D. Vicente, F. C. González, G. Bossis, and O. Volkova, "Normal force study in concentrated carbonyl iron magnetorheological suspensions," *Journal of Rheology*, vol. 46, no. 5, pp. 1295–1303, 2002.

[52] G. Liao, X. Gong, and S. Xuan, "Influence of shear deformation on the normal force of magnetorheological elastomer," *Materials Letters*, vol. 106, no. 9, pp. 270–272, 2013.

[53] G. Liao, X. Gong, S. Xuan, C. Guo, and L. Zong, "Magnetic-field-induced normal force of magnetorheological elastomer under compression status," *Industrial and Engineering Chemistry Research*, vol. 51, no. 8, pp. 3322–3328, 2012.